

Heat and mass transfer analysis of a coal particle undergoing pyrolysis

T. X. PHUOC and P. DURBETAKI†

The George W. Woodruff School of Mechanical Engineering, Georgia Institute of Technology,
Atlanta, GA 30332-0405, U.S.A.

(Received 7 April 1986 and in final form 2 April 1987)

Abstract—Heat and mass transfer are combined with kinetics to analyze a coal particle undergoing pyrolysis. The effects of particle size and surrounding temperature are investigated in terms of heat transfer while the effect of pressure is attributed to the competition of pyrolysis, secondary reaction, and the mass transport within the particle. At a high heat transfer rate, the weight loss is determined by the competition between pyrolysis and a secondary reaction. At a low heating rate, the contribution of internal mass transport becomes more pronounced. The weight loss is then determined by the competition between such internal transport and the deposition reaction.

1. INTRODUCTION

VOLATILE evolution from coal is governed by various factors. Among these are particle size, pressure, and heating rate. Kayihan and Reklaitis [1] and Kobayashi *et al.* [2] observed that 65–70% of the initial coal mass can be obtained as volatiles at heating rates up to 10^6 K s^{-1} and pyrolysis temperatures up to 2100 K. Anthony and Howard [3] reported values of the ratio of actual volatiles produced to the proximate volatiles, V^*/VM from 0.36 to 1.36, depending on coal type and operating conditions. In most cases, the heat transfer rate is fast compared to the chemical reaction. The variation of the volatile yield is indirectly due to the heating rate, which accelerates pyrolysis and increases the final temperature [4].

Very little experimental data is available concerning particle size dependence of volatile yields. Anthony and Howard [3] observed only a 2% decrease in weight loss of bituminous coal undergoing pyrolysis at 1000°C and 69 atm He, as particle diameters were increased from 70 to 1000 μm . However, they noted a decrease in the volatile yield from 59 to 44% of the initial mass at 60 atm H_2 . Similar effects were also reported by Gavalas and Wilks [5] and Desypris *et al.* [6].

The effect of pressure on the weight loss has been investigated by Anthony and Howard [3], Suuberg *et al.* [7], and Gavalas and Wilks [5] and has been reviewed by Wen and Tone [8]. Anthony and Howard [3] reported volatile yields of 50–55% of the weight of bituminous coal at 1000°C and 10^{-4} atm but only 34–40% at 100 atm.

The pronounced effect of pressure on the weight loss for a bituminous coal particle indicates competition among secondary reaction, hydrodynamic escaping of volatiles, and thermal decomposition of

coal. The volatiles produced can be classified as reactive and nonreactive. Non-reactive volatiles are low molecular weight hydrocarbons which can be transported away without loss due to a deposition reaction. Reactive volatiles are high molecular weight hydrocarbons which can redeposit, react with hydrogen to produce hydrogenated volatiles, escape via various pores to the surface and then diffuse into the surrounding gas. The reactive volatiles collected, therefore, depend on the competition of these mechanisms which in turn depend on pressure and particle size. At low pressure, transport rates are fast, and essentially all reactive volatiles escape the coal particle. At high pressure, the resistance against such escaping is great, making more reactive volatiles available for the deposition reaction. The reactive volatiles decrease but hydrogenated volatiles increase. Since the reactive volatiles dominate, on a mass basis, their reduction exceeds the increase of the gases; therefore, the total yield decreases.

Several attempts have been made to combine chemical kinetics and mass transfer to investigate the effects of pressure and particle size on weight loss. Such competition has been incorporated into the simple external film mass transport model by some authors [3]. Others [7, 9] have treated the transport essentially as evaporation. The process of escaping volatiles is not simple diffusion, however, but rather a complex process involving a time-dependent pore structure and hydrodynamic flow. The film mass transfer, in most cases, is very fast [10]. The effects of pressure and particle size on the yields must be due mainly to transport processes within the coal particle. Russel *et al.* [11] investigated the coupling mechanism of mass transport and chemical kinetics for coal hydro-pyrolysis in terms of diffusion and bulk flow within the particle; the authors did not discuss the combined effects of heat transfer and kinetics. Gavalas and Wilks [5] developed a model for intraparticle mass transfer in coal pyrolysis. Their flux relations are simi-

† Author to whom correspondence should be addressed.

NOMENCLATURE

c_p	specific heat at constant pressure	W_v	volatile evolution rate per unit mass of coal
D_{iK}	Knudsen diffusivity	VM	proximate volatile
D	binary diffusion coefficient	Y_i	mass fraction of species i .
E	activation energy	Greek symbols	
E_0	mean activation energy	α	pyrolysis coefficient
ΔH_s°	heat of pyrolysis	β_0	permeability
h_c	heat transfer coefficient	ϵ	void fraction
k	rate constant of pyrolysis	λ	thermal conductivity
k_0	frequency factor	μ	viscosity
k'	rate constant of deposition reaction	ξ	equation (21)
M_i	molal mass of species i	π_i	dimensionless group
\dot{m}_i	mass flow rate of species i	ρ	density
\dot{m}_i^*	equation (38)	σ	standard deviation of the mean activation energy
\dot{m}	total mass flow rate	ω	production rate.
P	pressure	Subscripts	
P^*	equation (21)	av	average
P_0	surrounding pressure	ch	char
r	radial coordinate	I	inert
r_p	pore radius	nrv	non-reactive volatile
r_s	particle diameter	P	pore
R	gas constant	p	particle
T	gas phase temperature	rv	reactive volatile
T_c	surrounding temperature	s	surface
T_p	particle temperature	v	volatile
$T_{p,0}$	initial particle temperature	0	initial.
t	time		
V	volatiles produced at time t		
V^*	volatiles produced at $t = \infty$		

lar to those of Russel *et al.* [11], but the tar production rate was treated as constant to simplify the analysis. Because it ignores the heat transfer mechanism, this model cannot predict whether effects of pressure and particle size are attenuated or accentuated when the particle temperature increases. Mills *et al.* [12] investigated the combined heat transfer and kinetics of a coal particle undergoing rapid pyrolysis. The effect of particle swelling was described in an empirical relation; secondary reactions were not discussed. James and Mills [13] investigated the pressure effect of coal particle pyrolysis using three different reaction schemes. With regard to the density of metaplast and semicoke at 1 and 10 atm ambient pressure, they showed that a model which allows for the competition among vaporization, and decomposition and cracking reactions can provide a good explanation of the experimentally observed pressure effect on the yield of volatiles from coal pyrolysis.

2. FORMULATION OF THE PROBLEM

Both heat and mass transfer affect the pyrolysis of a coal particle, yet previous studies have failed to consider the combined effect of heat transfer, mass transfer and kinetics. This paper, therefore, will focus

on these competing influences. Specifically, it will analyze a single spherical coal particle undergoing pyrolysis after sudden exposure to an inert atmosphere of helium. As shown in Fig. 1, the particle receives heat from the surrounding high temperature inert gas. As particle temperature increases, volatiles form and then escape via pores within region I to the particle surface where they diffuse into the surrounding regions II and III. As they escape, depending on pressure and particle size, these volatiles may redeposit via a deposition reaction, or they may fracture into lower molecular weight volatiles.

This investigation will focus primarily on region I, where the competition between diffusion transport, viscous transport, chemical kinetics of pyrolysis, and deposition occur. To examine these mechanisms requires knowledge of the coal particle structure, a complex configuration not entirely understood. Coal is a porous solid, its porosities varying between 2 and 20%, depending on type and seam. Some coals (e.g. subbituminous coals) retain a porous structure throughout the pyrolysis process. Others soften into a droplet, from which volatiles may escape as bubbles until resolidification occurs (e.g. softening high-volatile bituminous coals), and suffer a drastic structural transformation when particles are exposed to an elev-

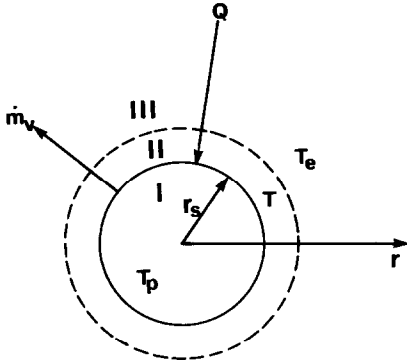


FIG. 1. Spherical particle undergoing pyrolysis: region I, intraparticle mass transport; region II, diffusion of mass and energy; region III, free stream.

ated temperature. It is clear that the two types of coal will not develop the same mechanism of mass transport mode. The analysis which follows, therefore, will be restricted to the coal particle as a porous sphere which more or less retains its structure as the reactions proceed.

2.1. Volatile transport

The transport of volatiles through the pores is expected to retard pyrolysis. This section of the study will therefore examine the fluid mechanics within the pore structure during pyrolysis. The model assumes (i) an isothermal particle, (ii) quasi-steady flux of volatiles, (iii) equal binary diffusivities, (iv) ideal gas volatiles, (v) one dimensional, (vi) constant properties, (vii) Fick's law valid in region II, and (viii) Lewis number of unity.

Assumption (ii) is based on the fact that mass transfer is fast and the changing pyrolysis rate can be equilibrated by the mass transport instantaneously. The validity of assumption (i) depends mainly on particle size and pyrolysis temperature. Gavalas and Wilks [5] reported that a variation of particle temperature did not exceed a few degrees for particle sizes up to 500 μm and a pyrolysis temperature up to 600°C. Sprouse [14] has indicated that for a particle size of the order of 100 μm , the temperature gradient within the particle is essentially negligible.

With these assumptions, the following diffusive conservation equations are written for the gas phase in region II:

mass

$$(1/r^2) \frac{d}{dr} (r^2 \dot{m}) = 0; \quad (1)$$

species

$$\frac{d}{dr} r^2 [\dot{m} Y_i - (\lambda/c_p)(dY_i/dr)] = 0; \quad \text{for } i = v, I; \quad (2)$$

momentum

$$P_0 = \text{constant}; \quad (3)$$

energy

$$\frac{d}{dr} r^2 [\dot{m} T - (\lambda/c_p)(dT/dr)] = 0. \quad (4)$$

Equations (1)–(4) are integrated with

$$r = r_s: \quad \dot{m}_{v,s} = \dot{m}_{v,s} Y_{v,s} - \rho D (dY_v/dr)_{r=r_s}; \quad (5)$$

$$T = T_s = T_p; \quad \lambda (dT/dr)_{r=r_s} = h_c (T_p - T_e) \quad (6)$$

$$r \rightarrow \infty: \quad Y_v = 0, \quad Y_I = 1, \quad T = T_e \quad (7)$$

and the result is

$$Y_{v,s} = 1 - \exp(-r_s \dot{m}_{v,s} / \rho D) \quad (8)$$

$$h_c = \dot{m}_{v,s} c_p / [\exp(r_s \dot{m}_{v,s} c_p / \lambda) - 1]. \quad (9)$$

Equations (8) and (9) will be used as boundary conditions for region I.

In region I, volatiles are produced and transported through the pores. The required conservation equations for mass balance are

$$(1/r^2) \frac{d}{dr} (r^2 \dot{m}_v) = \omega_v \quad (10)$$

$$(1/r^2) \frac{d}{dr} (r^2 \dot{m}_I) = 0 \quad (11)$$

where ω_v is the rate of volatile production due to pyrolysis.

The transport of volatiles through the pores is controlled either by diffusion or convection depending on pore size. The molar flux model developed by Mason and Evans [15] is adopted here. On a mass basis, the flux of volatiles and inert helium is

$$\dot{m}_i = -D_i \frac{d}{dr} (\rho Y_i) + \delta_i Y_i \dot{m} - (\gamma_i Y_i \rho \beta_0 / \mu) (dP/dr) \quad \text{for } i = v, I \quad (12)$$

where

$$\beta_0 = r_p^2 / 8 \quad (13)$$

$$(1/D_i) = (1/D_{iK}) + (1/D) \quad (14)$$

$$\delta_i = D_i / D \quad (15)$$

$$\gamma_i = 1 - \delta_i \quad (16)$$

$$D_{iK} = 9.7 \times 10^3 (T/M_i)^{1/2} r_p (\epsilon/3) \quad (17)$$

and the equation of state

$$P = \rho R T_p / M. \quad (18)$$

Equations (10)–(12) are solved subject to the following boundary conditions:

$$r = 0: \quad \lim (r^2 \dot{m}_i) = 0 \quad \text{for } i = v, I \quad (19a)$$

$$r = r_s; \quad P = P_0; \quad Y_{v,s} = 1 - \exp(-r_s \dot{m}_{v,s} / \rho D);$$

$$Y_{1,s} = 1 - Y_{v,s}. \quad (19b)$$

2.2. Solution

Using boundary condition (19a) and assumption (i), equations (10) and (11) are integrated to obtain

$$\dot{m}_v = \omega_v r / 3 \quad \text{and} \quad \dot{m}_1 = 0. \quad (20)$$

Define

$$\xi = r/r_s; \quad P^* = P/P_0; \quad m_v^* = \dot{m}_v / \omega_v r_s \quad (21)$$

$$\pi_1 = D_{vK} / D_{1K} \quad (22a)$$

$$\pi_2 = RT_p r_s^2 \omega_v / P_0 M D_{vK} \quad (22b)$$

$$\pi_3 = P_0 r_p^2 / 8 \mu D_{vK} \quad (22c)$$

$$\pi_4 = D_{vK} / D_v. \quad (22d)$$

Using equations (13)–(16) and (20)–(22), the dimensionless pressure and volatile mass fraction given by equation (12) becomes

$$\frac{dP^*}{d\xi} = \frac{-\pi_2 \xi}{3[1 + \pi_3 P^*(Y_v + \pi_1 Y_1)]} \quad (23)$$

$$\frac{dY_v}{d\xi} = \left\{ Y_v \left[\pi_1 + \frac{1 + \pi_3 P^*}{1 + \pi_3 P^*(Y_v + \pi_1 Y_1)} \right] - \pi_4 \right\} \frac{\pi_2 \xi}{3 P^*}$$

$$(24)$$

$$Y_1 = 1 - Y_v. \quad (25)$$

The dimensionless parameter π_2 is the ratio of characteristic times for diffusion and reaction, encompassing the effects of particle size and temperature. High values of π_2 indicate slow diffusion. Volatiles produced cannot be transported by diffusion. Low values of π_2 indicate that diffusion is fast and the volatiles produced will be carried away. The dimensionless parameter π_3 is the ratio of characteristic times for diffusion and forced flow. It is essentially dependent of pressure and pore size. Large values of π_3 indicate that the flow is viscous controlled, while small values indicate the flow is diffusive.

2.3. Results

Figure 2 illustrates the dimensionless pressure buildup, $P^*(0)$, as a function of π_2 and π_3 . A strong increase of $P^*(0)$ is found at high π_2 and low π_3 , and the internal pressure is approximately equal to that of the background at high π_3 and low π_2 . Since π_3 is the ratio of characteristic times for diffusion and forced flow, at low π_3 the transport is controlled mainly by diffusion. Under this condition, the development of the internal pressure is dependent on the competition between the volatile production rate and the rate of the diffusive transport.

In Fig. 3 the volatile mass fraction distributions within the particle as a function of π_3 are presented. At low π_3 , a high volatile mass fraction, Y_v , is obtained but it decreases as π_3 increases and it becomes constant throughout the particle for the case where $\pi_3 = 10^3$. These results indicate that the volatiles can-

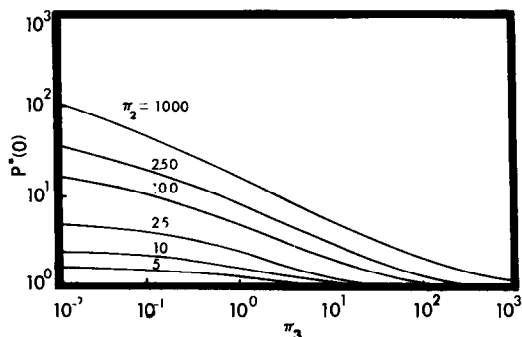


FIG. 2. Dimensionless pressure buildup as a function of π_2 and π_3 .

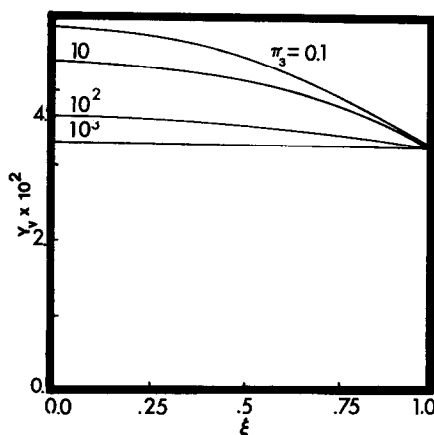


FIG. 3. Volatile mass fraction distribution as a function of π_3 ; $\pi_2 = 0.01$.

not escape from the coal particle by diffusive transport, therefore, the volatiles produced will remain in the pores, causing $P^*(0)$ to increase. The transport of volatiles can be accommodated essentially by viscous convection with increasing π_3 and hence a decrease of $P^*(0)$, as shown in Fig. 2. At low values of π_2 , the rate of volatile production is low compared to the rate of diffusive transport. Volatiles produced can be transported away and no significant increase of the internal pressure is obtained.

Figure 4 shows explicitly the effects of the ambient pressure and pore size on the internal pressure. A significant increase of the internal pressure is obtained at a low external pressure and for a pore size less than 10^{-5} cm. For a pore size greater than this value, the increase of the internal pressure is negligible. Simons [16], using pore tree theory, found that, depending on pore size, the volatile transport process undergoes transition directly from Knudsen diffusion to viscous convection. A significant increase of the internal pressure occurs in the Knudsen diffusion regime, and values of 3–10 atm above the ambient pressure were observed for bituminous coal. In the viscous convection regime, pressure buildup is not significant. Corresponding to a pyrolysis rate of 0.1 s, the transition pore size was of the order of 10^{-6} – 10^{-5} cm.

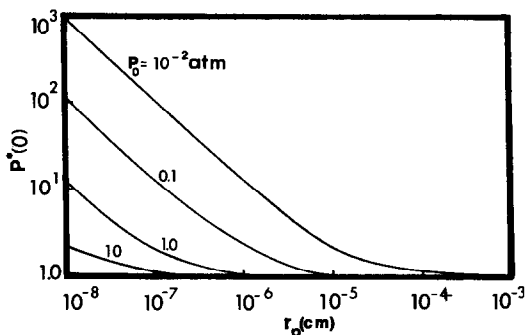


FIG. 4. Dimensionless pressure buildup as a function of r_p and P_0 .

This present calculation gives values of internal pressure from 3 to 12 atm above the ambient pressure, which ranges from 0.1 to 100 atm at $r_p = 1 \mu\text{m}$ as shown on Fig. 4. Comparing the information given by Fig. 4 with the transition size given by Simons [16] suggests that for $r_p > 10^{-5}$ cm, the variation of the internal pressure can be negligible throughout the particle.

James and Mills [13] studied the effect of the pressure level on coal particle pyrolysis using three different reaction schemes. When the competing vaporization and decomposition of metaplast was allowed, they found that at 1 atm vaporization dominates and the final value of semicoke density was only 1.84 kg m^{-3} . However, at 10 atm the semicoke density increased to 20.9 kg m^{-3} and the density of the metaplast was 2.5 times that at 1 atm. When cracking of volatiles was allowed, they obtained considerably more solid product semicoke deposited as the pressure level was increased from 1 to 10 atm. Thus they concluded that when the ambient pressure was low, the high vaporization rate created an overpressure, which in turn produced a high radial velocity and a low residence time for the volatiles in the particle. Hence the secondary reactions did not have enough time to develop significantly before the volatiles escaped from the particle. This present analysis predicts a similar increase of the internal pressure essentially in the pore range less than 10^{-5} cm where the volatiles cannot escape quickly from the particle. When the flow of volatiles is accommodated by the viscous transport, the internal pressure decreases to the ambient value. Thus the present prediction is consistent with that of James and Mills.

2.4. Conclusions

Based on the results cited above the following conclusions can be drawn:

(1) Since both π_2 and π_3 represent the competition among the rate of volatile production, viscous transport and the diffusive transport, these parameters are essentially dependent on heating rate, particle size and pressure. Therefore, a model which takes into account the competition between heat transfer, mass transfer and chemical processes within the coal particle will

make it possible to explain the effects of heating rate, particle size and pressure on the observed total yield of coal pyrolysis.

(2) The transport of volatiles through the pores is controlled by diffusion and viscous convection. Diffusion is dominant in the small pore sizes and viscous convection is dominant in larger pore sizes. The transition from diffusion to viscous transport will be determined by the pyrolysis rate and background pressure.

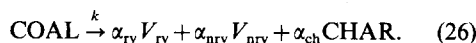
(3) The increase of internal pressure and the distribution of volatile mass fraction within the particle are significant only in the diffusion flow regime. In the viscous flow regime, such an increase of pressure and the variation of the volatile mass fraction within the coal particle are negligible.

3. COAL PYROLYSIS ANALYSIS

The transport of volatiles described in the previous section can be used to analyze the pyrolysis of a coal particle. To do so necessitates treating volatiles as reactive and non-reactive gases. Although in the diffusion flow regime, both reactive and non-reactive gases can be activated, only non-reactive gases can reach the particle surface. Reactive gases, initially produced as free radicals, can readily recombine with free radicals on the coal matrix. Therefore, this range of pore size can be excluded since information concerning the effects of pressure and particle size on the total weight loss of coal can be deduced only when the reactive volatiles are available for study. Only a pore size greater than $1 \mu\text{m}$ will be considered here. In this range the flow is dominated by viscous convection, and the internal pressure increase as well as the variation of reactive volatiles within the coal particle are neglected.

3.1. Kinetics of pyrolysis

The thermal decomposition of a coal particle is described as



The rates of volatile production are

$$\omega_{rv} = \rho_p (dV_{rv}/dt) - \rho k' Y_{rv} \quad (27)$$

$$\omega_{nrv} = \rho_p (dV_{nrv}/dt) \quad (28)$$

where $\rho k' Y_{rv}$ is the production rate due to the deposition reaction, and dV_{rv}/dt and dV_{nrv}/dt are the production rates of reactive and non-reactive volatiles due to pyrolysis, respectively. These volatile production rates are evaluated by

$$(dV_i/dt) = k(V_i^* - V_i) \quad \text{for } i = rv, nrv \quad (29)$$

where k , the rate constant, is given by Anthony and Howard [3] as

$$k = k_0 \int_0^{\infty} \exp(-E/RT_p) f(E) dE \quad (30)$$

and the Gaussian distribution of activation energies is

$$f(E) = [\sigma(2\pi)^{1/2}]^{-1} \exp[-(E-E_0)/2\sigma^2]. \quad (31)$$

3.2. Governing equations

Mass balance

$$(1/r^2) \frac{d}{dr} (r^2 \dot{m}_i) = \omega_i \quad \text{for } i = \text{rv, nrv} \quad (32)$$

$$(1/r^2) \frac{d}{dr} (r^2 \dot{m}_t) = 0. \quad (33)$$

Particle temperature

$$(dT_p/dt) = (3/\rho_p c_{p,p} r_s) [h_c(T_e - T_p) + \dot{m}_{v,s} \Delta H_s^\circ]. \quad (34)$$

Equations (29) and (32)–(34) are solved subject to

$$\text{at } t = 0, \text{ all } r: T_p = T_{p,0} \quad (35a)$$

$$V_i = 0 \quad \text{for } i = \text{rv, nrv, I} \quad (35b)$$

at $t \geq 0, r = 0$: $\lim (r^2 \dot{m}_i) = 0$

$$\text{for } i = \text{rv, nrv, I} \quad (36)$$

$r = r_s$: $Y_{i,s} = (\dot{m}_{i,s}/\dot{m}_{v,s}) [1 - \exp(-r_s \dot{m}_{v,s}/\rho D)]$

$$\text{for } i = \text{rv, nrv}. \quad (37)$$

3.3. Solution

Define

$$\dot{m}_i^* = \dot{m}_i / (r_s \rho_p k) \quad \text{for } i = \text{rv, nrv} \quad (38)$$

$$\pi_5 = \rho k Y_{rv} / \rho_p k (V_{rv}^* - V_{rv}) \quad (39)$$

$$\pi_6 = r_s^2 \rho_p k / 3\rho D. \quad (40)$$

Equation (32) becomes

$$(1/\xi^2) \frac{d}{d\xi} (\xi^2 \dot{m}_{rv}^*) = (V_{rv}^* - V_{rv})(1 - \pi_5) \quad (41)$$

$$(1/\xi^2) \frac{d}{d\xi} (\xi^2 \dot{m}_{nrv}^*) = (V_{nrv}^* - V_{nrv}). \quad (42)$$

These are integrated subject to equations (36) and (37) to obtain

$$\dot{m}_{rv}^* = (V_{rv}^* - V_{rv})(1 - \pi_5)\xi/3 \quad (43)$$

$$\dot{m}_{nrv}^* = (V_{nrv}^* - V_{nrv})\xi/3. \quad (44)$$

Because $r_s \dot{m}_{v,s}/\rho D$ is very small, the mass fraction of reactive volatiles can be calculated as

$$Y_{rv} = Y_{rv,s} = \pi_6 (V_{rv}^* - V_{rv})(1 - \pi_5). \quad (45)$$

The instantaneous rate of volatile evolution per unit mass of coal is

$$\begin{aligned} W_v &= \dot{m}_{v,s} (4\pi r_s^2) / (4/3) \rho_p \pi r_s^3 \\ &= k[(1 - \pi_5)(V_{rv}^* - V_{rv}) + V_{nrv}^* - V_{nrv}]. \end{aligned} \quad (46)$$

Parameter π_5 represents the competition between pyrolysis and the secondary reaction. It is assumed

that the temperature dependence on k' and k is of the same order. Therefore, π_5 depends essentially on pressure. Low π_5 values indicate a negligible contribution of the secondary reaction. The reactive volatile production is determined by π_6 . At high π_5 values, the contribution of the secondary reaction becomes pronounced. Both π_6 and π_5 determine the volatile yield.

3.4. Results

Figure 5 illustrates values of reactive volatile yield as a function of π_5 and π_6 . At low π_6 values all reactive volatiles produced can reach the surface. Due to fast mass transfer, the volatiles do not have time to react. At high values of π_6 , the yield of reactive volatiles decreases with increasing π_6 , indicating the contribution of the secondary reaction that causes the reactive volatiles to deposit back.

The curves in Fig. 5 may be compared with the results reported by Anthony and Howard [3], who found that 20% of the weight of coal converted to reactive volatiles at $P_0 = 10^{-4}$ atm but only 13.2% at $P_0 = 1$ atm. Parameter π_5 can be modeled as

$$\pi_5 = 1 - \exp(-0.415 P_0^{0.7}). \quad (47)$$

With equation (47), equations (29), (34) and (43)–(46) are integrated using $r_p = 1-1.5 \mu\text{m}$, $D = 0.37 \text{ cm}^2 \text{ s}^{-1}$, $c_p = c_{p,p} = 1.2-2.9 \text{ J g}^{-1} \text{ K}^{-1}$, $\rho_p = 1.3 \text{ g cm}^{-3}$ and appropriate kinetic data ($k_0 = 1.67 \times 10^{13} \text{ s}^{-1}$, $E_0 = 2.29 \times 10^5 \text{ J mol}^{-1}$, $\sigma = 7.2 \times 10^4 \text{ J mol}^{-1}$, $V_{rv}^* = 0.2$, $V_{nrv} = 0.372$) [3, 13]. It must be noted that since the binary diffusivity, D , is proportional to $1/P$ the product of ρD will be treated as a constant. Because the composition of the reactive volatiles has not been well defined their model formula has been assumed to be qualitatively in the form of $\text{C}_{12}\text{H}_8\text{O}_2$ [14]. The choice of the diffusivity coefficient is only a qualitative approximation of the average value for the compound whose molecular weight is that of the above formula. Results encompassing the effects of r_s , T_e and P_0 are shown in Figs. 6–10.

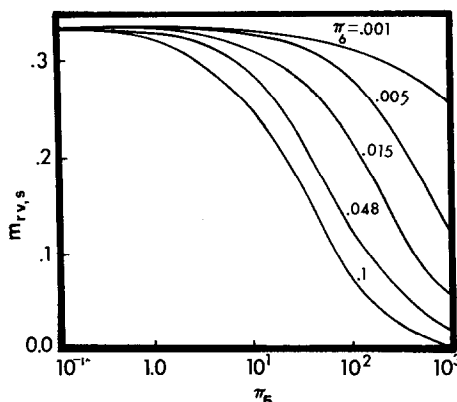


FIG. 5. Dimensionless yield of a reactive volatile as a function of π_5 and π_6 .

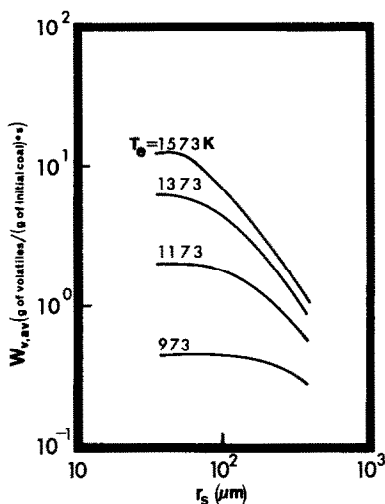


FIG. 6. Effect of particle size on the average rate of volatile evolution: $P = 1$ atm.

Figures 6–9 show the average value of pyrolysis rate as a function of r_s , T_e and P_0 . $W_{v,av}$ is independent of r_s , for $r_s < 50 \mu\text{m}$ at all T_e . However, at low T_e , the particle-size independence of $W_{v,av}$ exists even for higher r_s . For all cases, $W_{v,av}$ increases with increasing temperature. It is clear from this result that the kinetic limit with no particle size dependence exists at low T_e . However, at high T_e , this limit is obtained only at small r_s . For the large particle sizes, the process is subject to heat transfer control, which depends on the total amount of $(T_e - T_p)$ and which is limited only at values of $T_e > 1573$ K.

Mills *et al.* [12] studied rapid pyrolysis of a coal particle, including the swelling effect, and predicted the ultimate weight loss to be independent of particle size. The particle size influences only the time required to complete the devolatilization. With the average rate of pyrolysis expected to be inversely proportional to particle diameter squared, the investigators predicted

the kinetic limitation for low particle size and low T_e . For particle sizes from 295 to 833 μm and $T_e = 1250$ K, they predicted temperature time responses equal to 1060 and 990 K, respectively. They argued that the effective ΔT for heat transfer varies appreciably with particle size and therefore T_e must be higher than 1250 K before a true heat transfer limitation can be observed. Thus, their findings are in accord with the prediction of this paper.

Figures 7 and 8 show $W_{v,av}$ as a function of pressure with r_s and T_e as variable parameters, respectively. For all ranges of pressure, the pyrolysis rate increases with increasing T_e and decreasing r_s . However, at low pressure it is essentially independent of pressure and strongly dependent on pressure at high pressure. This effect of pressure is neither attenuated nor accentuated with increasing temperature and particle size.

The above results are best explained by relating the particle size and surrounding temperature to the heat transfer rate. The particle temperature, which influences the balance between kinetics and mass transfer, is determined by the thermal response of the particle which, in turn, is controlled by the heat transfer rate. The latter is determined by the surrounding temperature and particle size. Figure 9 shows the average heat transfer rate as a function of particle size and surrounding temperature. It increases with increasing T_e and decreasing r_s .

An increase in the heat transfer rate leads to fast particle-temperature response and consequently results in an accelerated pyrolysis rate. The process is, therefore, completed in a shorter time as shown in Fig. 10, where the instantaneous yield of volatiles as a function of r_s is illustrated. Due to a high rate of pyrolysis, the internal resistance against the hydrodynamic transport of mass can be negligible. The process is essentially kinetic controlled and the volatile yield is determined by the competition between the pyrolysis and the secondary reaction. At low pressure, the contribution of the secondary reaction is insign-

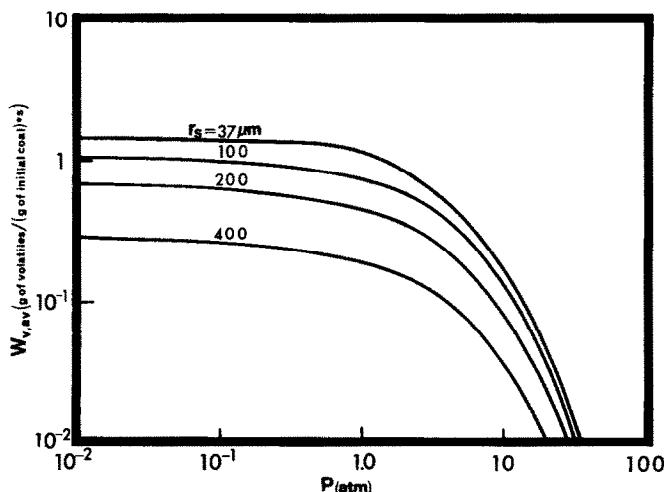


FIG. 7. Average rate of reactive volatile evolution as a function of pressure and particle size: $\Delta H_s^\circ = -245.3 \text{ J g}^{-1}$, $T_e = 1273$ K.

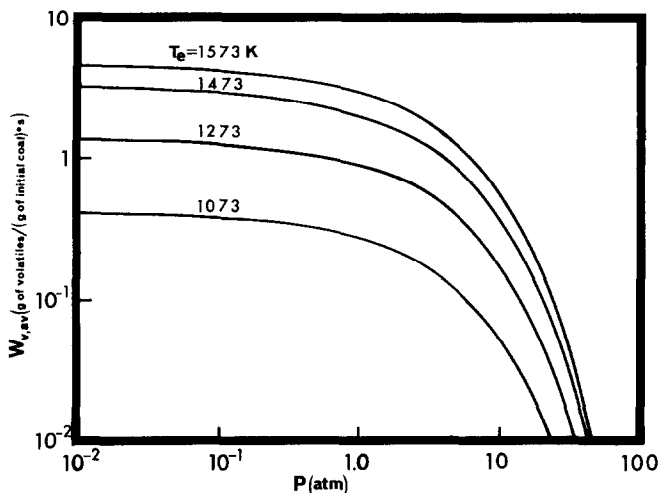


FIG. 8. Average rate of reactive volatile evolution as a function of pressure and temperature: $\Delta H_s^\circ = -245.3 \text{ J g}^{-1}$, $r_s = 63 \mu\text{m}$.

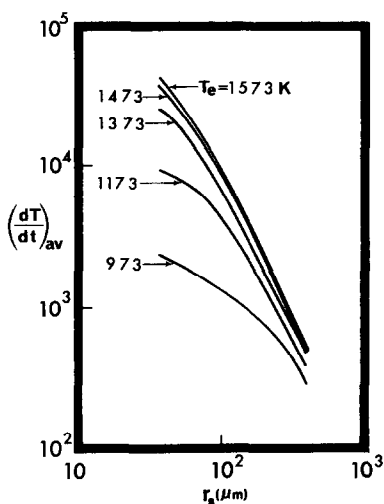


FIG. 9. Effect of particle size on average heat transfer rate: $P = 1 \text{ atm}$.

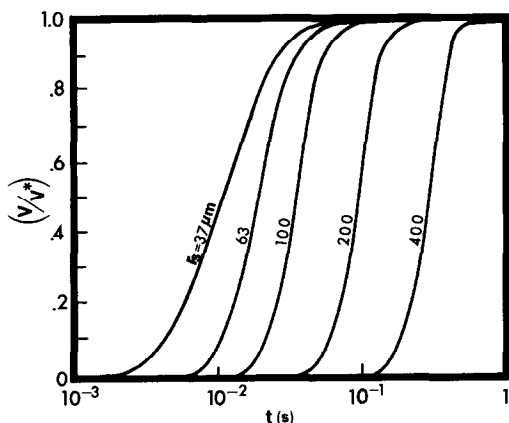


FIG. 10. Effect of particle size on coal conversion: $\Delta H_s^\circ = -245.3 \text{ J g}^{-1}$, $T_e = 1273 \text{ K}$, $P = 1 \text{ atm}$.

nificant and the evolution rate is independent of pressure. As pressure increases, the competition favors the secondary reaction. The evolution rate decreases with increasing pressure.

4. CONCLUSION

A study of the combined effects of heat and mass transport in the pyrolysis of a coal particle shows that heat and film mass transfer rates are fast compared to chemical reaction and do not affect the mass loss. The heat transfer rate accelerates pyrolysis, and the process is thus completed in a shorter time and at a higher final temperature. An increase in the surrounding temperature and a decrease in particle size produces a higher heating rate, which in turn increases the rate of volatiles and overcomes the diffusive transport within the particle. The mass loss is determined essentially by the competition between pyrolysis and the secondary reaction. At a low heating rate, the contribution of the mass transport becomes more pronounced, and the mass loss is determined solely by the competition between the internal transport of mass and the deposition reaction.

REFERENCES

1. F. Kayihan and G. V. Reklaitis, Modeling of staged fluidized-bed coal pyrolysis reactor, *Ind. Engng Chem. Process. Des. Dev.* **19**, 15-23 (1980).
2. H. Kobayashi, J. B. Howard and A. F. Sarofim, Coal devolatilization at high temperature, Sixteenth Symposium (International) on Combustion, pp. 411-425. The Combustion Institute, Pittsburgh, Pennsylvania (1977).
3. D. B. Anthony and J. B. Howard, Coal devolatilization and hydrogasification, *A.I.Ch.E. JI* **22**, 625-656 (1976).
4. V. T. Ciuryla, R. F. Weimer, D. A. Bivans and S. A. Motika, Ambient pressure thermogravimetric characterization of four different coals and their chars, *Fuel* **58**, 748-754 (1979).

5. G. R. Gavalas and K. A. Wilks, Intraparticle mass transfer in coal pyrolysis, *A.I.Ch.E. JI* **26**, 201–212 (1980).
6. J. Desypris, P. Murdock and A. Williams, Investigation of the flash pyrolysis of some coals, *Fuel* **61**, 807–816 (1982).
7. E. M. Suuberg, W. A. Peters and J. B. Howard, Product composition and formation kinetics in rapid pyrolysis of pulverized coal. Implication for combustion, Seventeenth Symposium (International) on Combustion, pp. 117–130. The Combustion Institute, Pittsburgh, Pennsylvania (1979).
8. C. Y. Wen and S. Tone, *Coal Conversion Reaction Engineering*, ACS Symp. Series, No. 72, p. 56. Hemisphere, Washington, DC (1978).
9. P. E. Unger and E. M. Suuberg, Modeling the devolatilization behavior of a softening bituminous coal, Eighteenth Symposium (International) on Combustion, pp. 1203–1211. The Combustion Institute, Pittsburgh, Pennsylvania (1981).
10. G. R. Gavalas, *Coal Pyrolysis*, p. 77. Elsevier, New York (1982).
11. W. B. Russel, D. A. Saville and M. I. Greene, A model for short resident time hydrolysis of single coal particles, *A.I.Ch.E. JI* **25**, 65–80 (1979).
12. A. F. Mills, R. K. James and D. Antoniak, Analysis of coal particle undergoing rapid pyrolysis. In *Future Energy Production Systems* (Edited by J. C. Dentons and N. H. Afgan), Vol. II, p. 537. Hemisphere, Washington, DC (1976).
13. R. K. James and A. F. Mills, Analysis of coal particle pyrolysis, *Lett. Heat Mass Transfer* **3**, 1–12 (1976).
14. K. M. Sprouse, Modeling pulverized coal conversion in entrained flows, *A.I.Ch.E. JI* **26**, 964–974 (1980).
15. E. A. Mason and R. B. Evans III, Graham's laws: simple demonstrations of gases in motion, *J. Chem. Educ.* **46**, 358–364 (1969).
16. G. A. Simons, Coal pyrolysis II. Species transport theory, *Combustion Flame* **55**, 181–194 (1984).

ANALYSE DU TRANSFERT DE CHALEUR ET DE MASSE POUR UNE PARTICULE DE CHARBON EN COURS DE PYROLYSE

Résumé—Le transfert de chaleur et de masse est combiné à la cinétique pour analyser la pyrolyse d'une particule de charbon. Les effets de la taille de la particule et de la température ambiante sont étudiés en fonction du transfert de chaleur tandis que l'effet de la pression est attribué à la compétition de la pyrolyse, de la réaction secondaire et du transfert de masse dans la particule. Aux grands flux de chaleur transféré, la perte de masse est déterminée par la compétition entre la pyrolyse et la réaction secondaire. Aux faibles flux de chaleur, la contribution du transfert de masse interne devient plus prononcée; la perte de masse est alors déterminée par la compétition entre ce transfert interne et la réaction de déposition.

UNTERSUCHUNGEN ZUM WÄRME- UND STOFFÜBERGANG BEI DER PYROLYSE VON KOHLEPARTIKELN

Zusammenfassung—Die Gesetze der Wärme- und Stoffübertragung werden mit kinetischen Beziehungen verknüpft, um die Pyrolyse von Kohlepartikeln zu analysieren. Es wird die Beeinflussung des Wärmeübergangs durch die Partikelgröße und die Umgebungstemperatur untersucht, während die Druckeinflüsse der Wechselwirkung zwischen Pyrolyse, Sekundärreaktion und Stofftransport innerhalb der Partikel zugeordnet werden. Bei hohen Wärmeströmen wird der Gewichtsverlust durch die Wechselwirkung zwischen Pyrolyse und Sekundärreaktion bestimmt. Bei niedriger Heizleistung nimmt der Einfluß des inneren Stofftransports zu. Der Gewichtsverlust wird dann durch die Wechselwirkung zwischen innerem Transport und Ablagerungsreaktionen bestimmt.

АНАЛИЗ ПРОЦЕССОВ ТЕПЛО-И МАССООБМЕНА ПРИ ПИРОЛИЗЕ УГОЛЬНОЙ ЧАСТИЦЫ

Аннотация—Проводится совместный анализ кинетики и тепломассообмена угольной частицы в процессе пиролиза. Влияние размера частиц и температуры окружающей среды изучается для случая теплообмена, а влияние давления связывается с пиролизом, вторичной реакцией и массопереносом внутри частицы. При большой интенсивности теплообмена потеря веса определяется пиролизом и вторичной реакцией. При небольшой скорости нагрева более существенен вклад внутреннего массопереноса. В этом случае потеря веса происходит за счет внутренних процессов переноса и реакции осаждения.